# Two-Dimensional Supramolecular Polymers Embodying Large Unilamellar Vesicles in Water

Shigui Chen, Shane M. Polen, Lu Wang, Makoto Yamasaki, Christopher M. Hadad, and Jovica D. Badjić*

Department of Chemistry and Biochemistry, The Ohio State University, 100 West 18th Avenue, Columbus, Ohio 43210, United States

**S** *Supporting Information*

**ABSTRACT:** We hereby describe a strategy for obtaining novel topological nanostructures consisting of dual-cavity basket **1**, forming a curved monolayer of large unilamellar vesicles in water (CAC < 0.25 μM), and bivalent guests **4/5** populating the cavities of such bolaamphiphilic hosts. On the basis of the results of $^1H$ NMR spectroscopy, electron microscopy, and dynamic light scattering measurements, we postulated that divalent guest molecules **4/5** cover the curved vesicular surface in a lateral fashion to satisfy the complexation [2 + 2] valency and thereby give stable two-dimensional supramolecular polymers $[1 \subset 4]_n$ and $[1 \subset 5]_n$. The results of experimental studies are also supported with coarse-grained molecular dynamics simulations and molecular mechanics. Our discovery about the assembly of novel vesicular structures could be of interest for stabilization/functionalization of liposomal surfaces as well as detection of polyvalent molecules and removal of targeted substances from aqueous environments.
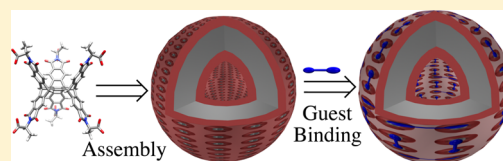
## INTRODUCTION

The preparation of more effective chemosensors, catalysts, and artificial scavengers is, in part, contingent upon our fundamental understanding of the recognition of small molecules and ions.[1−7] Over the years, chemists have designed various concave hosts[8−11] and probed the role of their dynamics, electron distribution, and shape for trapping targeted compounds.[12−16] As originally advocated by Cram,[17] the preorganization and complementarity[18] of host−guest pairs is essential for the formation of stable complexes with the effect of solvation playing an important role.[19−21] In line with this, noncovalent interactions are said to be "context dependent"[22−24] and one would, typically, use experimental methods to probe the stability and persistence[16,25−29] of host−guest complexes before establishing a reliable computational model to account for the results. In particular, elucidating the mode of action of polyvalent compounds and understanding the necessary topological features of their complexes continues to be an arduous task.[30−34] Multivalent interactions have thus been shown to be stronger than the corresponding monovalent interactions[35] and are of great value for the preparation of functional materials and therapeutics.[36−38] In this vein, the formation of supramolecular polymers[39] relies on establishing strong and multiple contacts[40] between molecular components to give long and dynamic linear chains.[41] Accordingly, we hereby present results on multivalent[35] assembly of divalent basket **1** (Figure 1A) and guests **4−5** (Figure 1B) in water. Importantly, bolaamphiphilic cavitand **1** forms stable and large unilamellar vesicles (LUV) capable of trapping bivalent **4/5** in the vesicular layer. The topology of the assembled host/guest pairs is unprecedented, giving rise to curved and finite supramolecular polymers encircling the space.[42,43]

## RESULTS AND DISCUSSION

Recently, we described the recognition characteristics of dual-cavity **1** (Figure 1A), carrying six (S)-alanine residues at the entrance of its two juxtaposed cavities (289 Å$^3$).[44] The bivalent basket was found to bind a single molecule of large guest **2** (241 Å$^3$, Figure 1A) to give the equimolar [**1**⊂**2**] complex ($K_1$ = 1.45 ± 0.40·10$^4$ M$^{-1}$), while one or two molecules of small **3** (180 Å$^3$, Figure 1A) to form binary [**1**⊂**3**] and ternary [**1**⊂**3**$_2$] complexes ($K_1$ = 7910 M$^{-1}$ and $K_2$ = 2374 M$^{-1}$) in water. To explain the observed allosteric mode of action,[45] we suggested that larger molecule **2** effectively populates a single cavity of **1**, thereby forming C−H···π contacts[46] with all three of the aromatic walls. Consequently, the adjacent cavity decreases in size and becomes more rigid, thus preventing additional encapsulations (Figure 1A). On the contrary, smaller guest **3** interacts with only one or two aromatic walls of the basket's cavity to render the singly occupied host flexible enough to undergo additional structural changes necessary for receiving another guest of the same type (Figure 1A). On the basis of these results, we wondered: will bivalent guest **4** (Figure 1B), an extended variant of monovalent **3**, bind to bivalent basket **1** to give linear supramolecular polymer $[1 \subset 4]_n$ of AA−BB type (Figure 1B)?[47,48]

To test our hypothesis, we began by examining the aggregation of dual-cavity **1** in water. A solution of **1** (0.2 mM in H$_2$O) was thus deposited on a copper grid and the thin film of cavitands was imaged with transmission electron microscopy (TEM); note that the solution of **1** was prepared without any sonication. Apparently, dual-cavity **1** organized into large unilamellar vesicles (Figure 2A) with an approximate
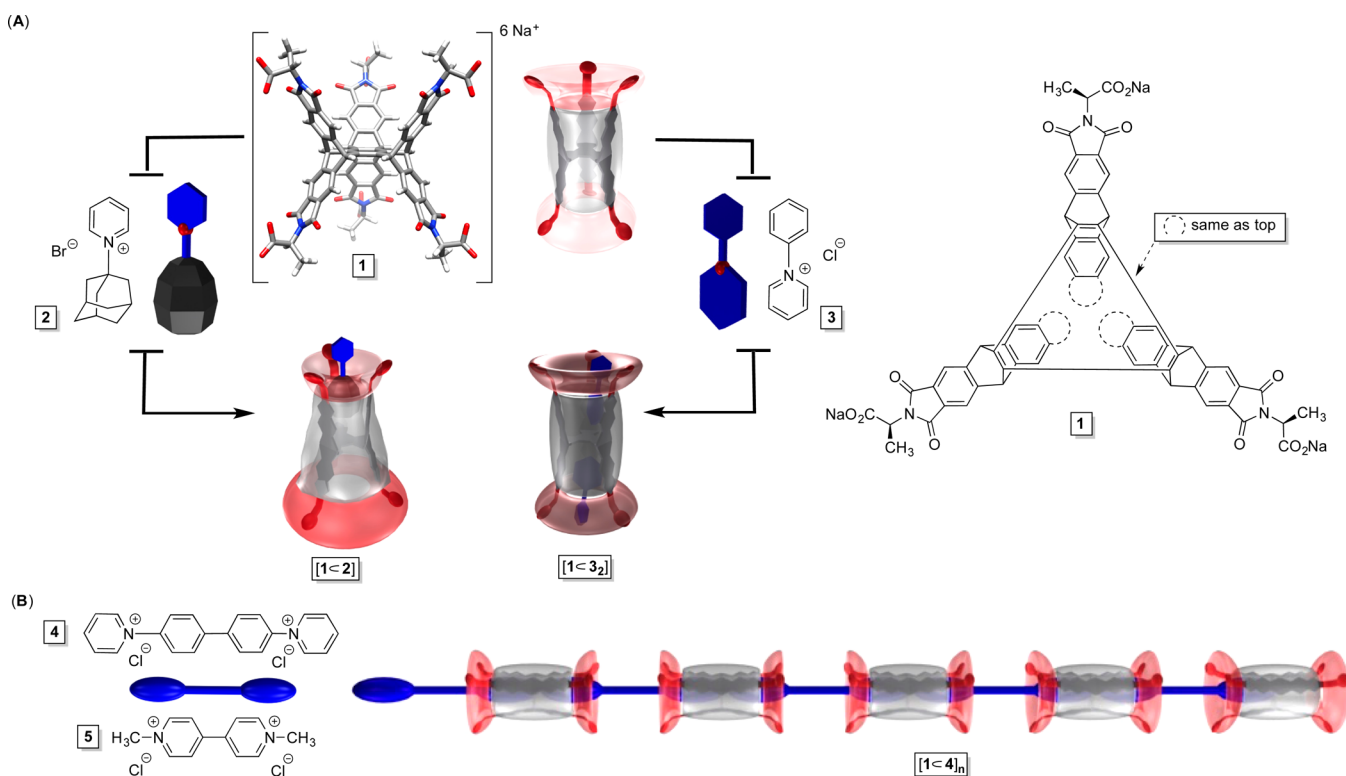
**Figure 1.** (A) A stick representation of dual-cavity **1** (chemical structure is shown on right) and chemical structures of monovalent **2**/**3** complexing the basket host. (B) A schematic representation of bivalent **4**/**5** guests forming linear AA−BB supramolecular polymers $[1\subset4]_n$ and $[1\subset5]_n$.[46]

diameter of 150−200 nm: cryogenic TEM (cryo-TEM) measurements revealed that the width of the bilayer "membrane" is about 2.9 nm (Figure 2A). Furthermore, dynamic light scattering (DLS) measurements of **1** suggested the existence of nanosized particles whose size distribution (PDI = 0.4, Figure 2B) is centered on $D_H$ = 230 nm, in agreement with the electron microscopy measurements. With the shape of a double truncated cone,[49−51] we deduced that bolaamphiphilic **1** packs into unilamellar vesicles by positioning the six negatively charged carboxylates at the water boundary so that the hydrophobic frameworks become "buried" and away from the polar environment:[51,52] the width of the vesicular monolayer, composed of baskets, is computed to be ~2 nm (Figure 2D) and therefore comparable to the membrane thickness estimated with cryo-TEM measurement (Figure 2A). Then, we used coarse-grained molecular dynamics (MD, Martini force field)[53] to examine the dynamics and stability of vesicles consisting of dual-cavity **1** (Figure 2C/D) while fully solvated in water and with sodium counterions (see Table S1 for calibration details). The coarse-grained methods are based on a mapping process whereby several heavy atoms are grouped and represented with a single interaction center—a "bead". In the case at hand, we used 36 beads to depict dual-cavity **1** (Figure 2C): 700 baskets were needed to build a vesicle of 20 nm in diameter, while a 50 nm vesicle included 3100 baskets— along with thousands of water molecules and sodium counterions in the simulations. Importantly, the monolayer of **1** stayed practically unperturbed in water, with minute lateral movements of basket molecules for the duration of the simulation (1.5 $\mu$s, Figure 2D). Furthermore, the size of cavities at the outer vesicular surface (0.26 ± 0.02 nm²) remained almost identical as those lining the inner side of the vesicular membrane (0.28 ± 0.02 nm²).

To examine the stability of vesicles, we completed ¹H NMR dilution study of **1** (Figure S1). The absence of the sharpening of resonances with dilution (Figure S1) suggested that critical aggregation concentration (CAC) of dual-cavity **1** in water ought to be lower than 10 $\mu$M. We also recorded fluorescence spectra of pyrene in the presence of the basket **1** (0.25 to 20 $\mu$M, Figure S2/3) to obtain evidence supporting the existence of vesicles at a concentration of **1** equal or greater than 0.25 $\mu$M. In particular, the ratio of the intensity of two pyrene's fluorescent bands ($I_I$ at 373 nm and $I_{III}$ at 384 nm; $I_{ex}$ = 334 nm)[54] underwent a small increase, but not a decrease,[55,56] upon an incremental addition of a standard solution of **1** to pyrene with a quenching of its fluorescence (Figure S2). On the basis of the literature,[57] we reasoned that the pyrene fluorophore was, upon entering the vesicular layer, undergoing a photo-induced electron transfer (PET) with the reduction of the phthalimide groups within the basket's framework.[58] As the results of the titration also indicated the formation of 1:1 stoichiometric complex ($[1\subset$pyrene$]$, Figure S3), we deduce the existence of visicles at $[1]$ > 0.25 $\mu$M.

The addition of 1-(1-adamantyl)pyridinium bromide **2** (4.0 mM) to vesicular **1** (0.2 mM in water) led to the formation of vesicles ($D_H$ = 250 nm, Figure 3A) consisting of binary $[1\subset2]$ complexes. Indeed, the results of DLS measurements indicated the predominant formation of nanosized particles whose size distribution (PDI = 0.6) was centered at $D_H$ = 325 nm (Figure 3A). As discussed earlier,[44] the formation of $[1\subset2]$ leads to a contraction of the cavity of **1**, in order to accommodate the guest, while causing the juxtaposed binding pocket to expand; note that the reported binding data[44] apply to guest **2** complexing baskets already assembled into vesicles. Accordingly, we presume that guest **2** equally populates both the inner and outer cavities of dual-cavity **1**, arranged within two-
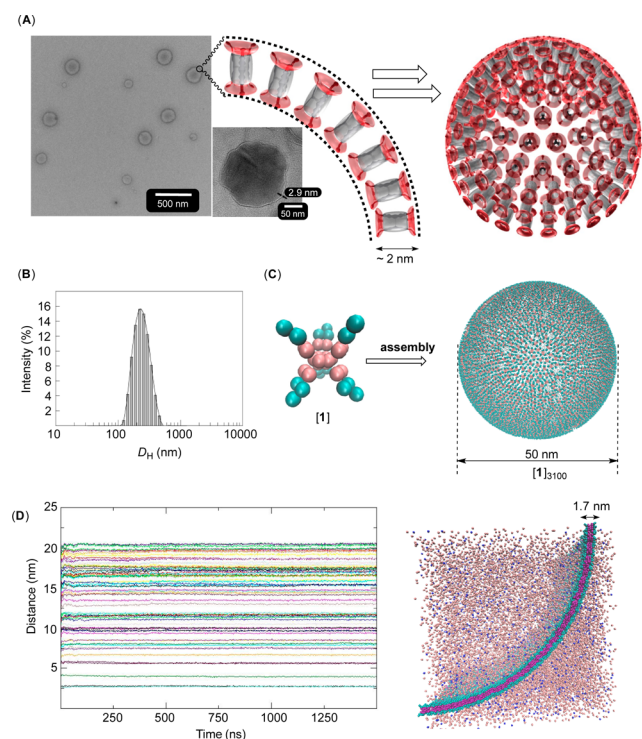
**Figure 2.** (A) TEM image of a solution of **1** (0.2 mM in H₂O), deposited on a copper grid and stained with uranyl acetate; cryo-TEM image of **1** (0.1 mM), showing a single vesicle with ca. 2.9 nm thick membrane corresponding to a monolayer of **1**. (B) A size distribution of **1** (0.2 mM in H₂O) was obtained from DLS measurements at 298.0 K. (C) Coarse-grained MD simulations of basket **1** in water revealed that 20 (not shown) and 50 nm vesicles would remain stable for 1.5 μs. (D) The variable distance of one basket from 70 others (from MD) is plotted over 1.5 μs. (Right) A cross section of the coarse-grained 20 nm vesicle with ca. 1.7 nm thickness.
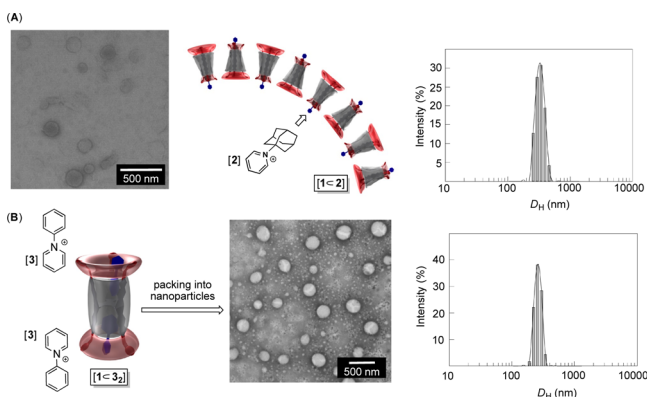


**Figure 3.** (A) TEM image of a solution of **1** (0.2 mM in water) containing guest **2** (4.0 mM) deposited on a copper grid and stained with uranyl acetate. (Right) A size distribution of **1** (0.2 mM in H₂O) containing guest **2** (4.0 mM) was obtained from DLS measurements at 298.0 K. (B) TEM image of a solution of **1** (0.2 mM in water) containing guest **3** (4.0 mM) deposited on a copper grid and stained with uranyl acetate. (Right) A size distribution of **1** (0.2 mM in H₂O) containing guest **3** (4.0 mM) was obtained from DLS measurements at 298.0 K.

dimensional and curved vesicular monolayer, to avoid creating van der Waals strain resulting from the exclusive packing on either inner or outer surfaces (Figure 3A). On the contrary, the addition of 1-(1-phenyl)pyridinium bromide **3** (4.0 mM) to

vesicular **1** (0.2 mM) led to seemingly the formation of nanoparticles ($D_H$ = 250 nm, Figure 3B) lacking the internal water reservoir and containing binary [**1⊂3**] (10%) and ternary [**1⊂3₂**] (89%) complexes; note that from the microscopy image (Figure 3B), it is difficult to distinguish any bilayer membrane of the nanosized structures having the interior with a uniform appearance. Presumably, populating both cavities of **1** with **3** should appreciably change the host's shape to trigger a repacking[49,50] of the assembly into another type of nano-structured material.[59]

Finally, we set to examine the interaction of bivalent **4** with host **1** (Figure 4A). An incremental addition of **4** (12.0 mM) to
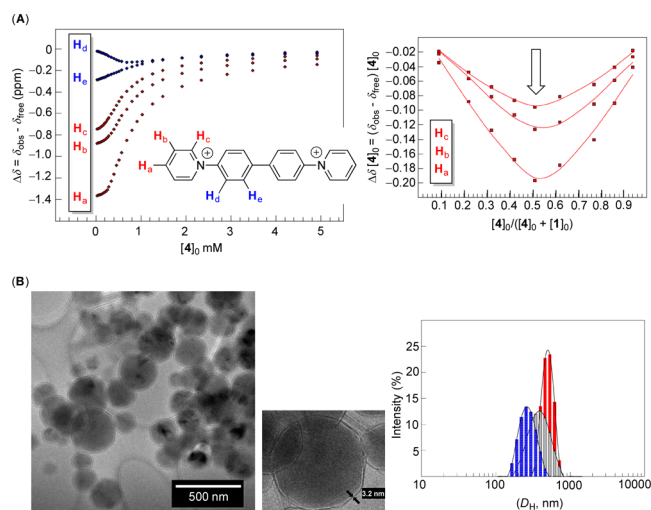


**Figure 4.** (A) The observed ¹H NMR chemical shifts ($\Delta\delta = \delta_{observed} - \delta_{free}$, ppm) of protons in **4** were obtained upon an incremental addition of its 12.0 mM solution to **1** (0.3 mM in D₂O) at 298.0 K. (Right) The Job plot corresponding to the formation of [**1⊂4**] in D₂O at 298 K with [**1**]₀ + [**4**]₀ = 0.3 mM. (B) Cryo-TEM images of a solution of **1** (0.1 mM in H₂O) containing **4** (0.1 mM). (Right) Size distributions of **1** (0.2 mM in H₂O) containing 1 (red), 5 (gray), and 20 (blue) molar equivalents of **4** were obtained from DLS measurements at 298.0 K.

D₂O solution of **1** (0.3 mM) was followed with ¹H NMR spectroscopy (600 MHz, Figure S4) to exhibit the perturbation of resonances of both compounds. In particular, the signals corresponding to protons $H_{a/b/c}$ of the pyridinium ring in **4** underwent a greater upfield shift ($\Delta\delta = \delta_{obs} - \delta_{free} = -0.74$ to $-1.36$ ppm, Figure 4A) than $H_{d/e}$ ($\Delta\delta = -0.12$ to $-0.26$ ppm, Figure 4A) to denote the entrapment of the pyridinium moiety. In fact, both pyridinium groups of **4** must be occupying the host's cavities since the degree of diamagnetic shielding of the guest's $H_a$ proton ($\Delta\delta = -1.4$ ppm, Figure 4A), by the host's surrounding aromatics, is comparable to the most perturbed protons of **2** and **3** ($\Delta\delta = -1.3$ to $-1.6$ ppm, Figures S5 and S6) within dual-cavity **1**.[44] The method of continuous variation,[60] furthermore, disclosed a bell-shaped curve peaking at 1:1 host–guest ratio (Figure 4A) to indicate the formation of equimolar [**1⊂4**] in solution. The electron microcopy measurements revealed the formation of vesicles (Figure 4B) with a distribution of sizes (PDI = 0.63, DLS) centered at 496 nm (Figure 4B). Importantly, these vesicles are unilamellar with ~3.2 nm thick membrane (Figure 4B) akin to the one observed for the host itself (2.9 nm, Figure 2A). It follows that a monolayer of [**1⊂4**] complexes must pack in a mode similar to the host (Figure 2A). Moreover, vesicular [**1**] is upon the
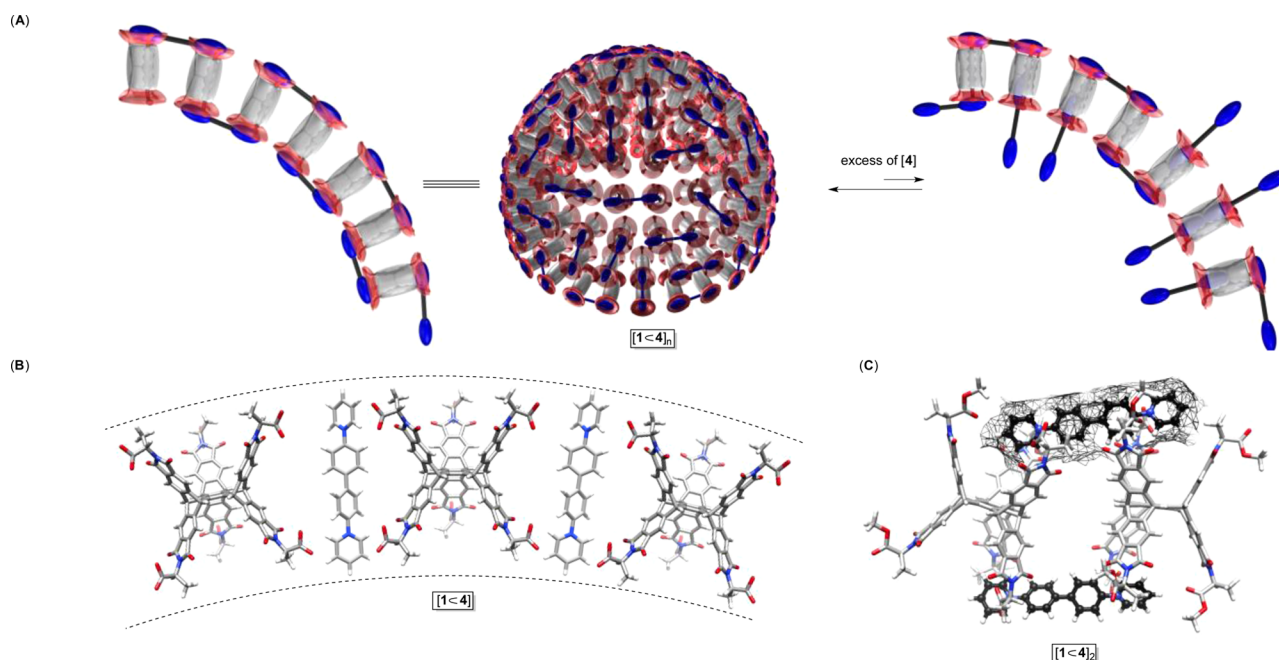
**Figure 5.** (A) A schematic representation of the postulated assembly of the proposed two-dimensional supramolecular polymer $[1{\subset}4]_n$. (B) A representation of vertical insertion of **4** into a curved monolayer of **1** to give $[1{\subset}4]_n$. (C) Energy-minimized (MMFFaq, Spartan) structure of $[1{\subset}4]_2$, with each basket having two carboxylates and four methyl ester groups; see also Figure S8.

addition of guest **4** changing its apparent size from $D_H = 230$ nm (Figure 2B) to $D_H = 496$ nm in $[1{\subset}4]_n$ to indicate a molecular reorganization following the recognition process in which hosts and guests pack into the observed larger vesicles. In light of the experimental results, the originally anticipated formation of linear supramolecular polymers (Figure 1B) became difficult to envision. *How do guest molecules 4 fit into the curved monolayer comprising dual-cavity 1 to give equimolar complexes with both of the guest's pyridinium groups entrapped?* To address the question, we first considered a scenario whereby the assembled **1** receives pyridinium units emanating from **4** to give supramolecular polymer $[1{\subset}4]_n$ resembling the linear one (Figure 1B) although with guests residing perpendicular with respect to the hosts (Figure 5A). If such one-dimensional assembly is extended to two dimensions (Figure 5A), one obtains a finite supramolecular polymer with curved topology. In this way, the complexation stoichiometry stays 1:1 while the polyvalency becomes satisfied: both cavities in the assembled **1** receive pyridinium units emanating from **4**. Another plausible scenario for the observed complexation consists of inserting guest molecules in the vesicular membrane such that guests span the monolayer of **1** with the positive sites in a close proximity of negatively charged carboxylates from the hosts (Figure 5B). Importantly, ^{1}H NMR titration results (Figure 4A) are more in line with horizontal (Figure 5A) than vertical (Figure 5B) alignment of guest molecules with respect to the vesicular membrane composed of **1**. As discussed earlier, a greater diamagnetic shielding of the resonances corresponding to $H_{a/c}$ than $H_{d/e}$ protons in **4** suggests the inclusion of the pyridinium rings in the cavity of **1**; in fact, similar magnetic perturbations of proton resonances were already measured for a guest bridging two adjacent and aromatic cavities of a host (see Figure S7).[61] On the contrary, the vertical insertion of guests **4** (Figure 5B) is expected to show a smaller perturbation of the pyridinium $H_{a/c}$ while greater shielding of $H_{d/e}$ resonances. A computational study of the $[1{\subset}4]_2$ complex (MMFFaq,

Spartan), with energy corrections for water solvation, revealed a family of comparable conformers (Figure 5C) with greater than 97% of the Boltzmann population distribution at 298 K (Monte Carlo conformational search, 500 steps; see Figure S8). The guest molecules in $[1{\subset}4]_2$ connect the hosts by adopting horizontal positions and protruding between the baskets' aromatic arms. These computations thus gave credence to the proposed and plausible model in which the vesicular layer of $[1{\subset}4]_n$ embodies dual-cavity **1** interwoven with bivalent **4** into a two-dimensional and curved supramolecular polymer (Figure 5A). To further examine the proposition, we reasoned that the degree of the suggested networking should be a function of the host−guest ratio.[41] That is to say, an excess of either host or guest could act as a "chain stopper" to disrupt the proposed meshwork pattern (Figure 5A): note that for AA−BB-type supramolecular polymers, a nonstoichiometric ratio of the complementary components brings about the fragmentation of longer chains.[62] Indeed, the results of DLS measurements of aqueous mixtures of **1** (0.2 mM in $H_2O$) and **4**, in the proportion of 1:1, 1:5, and 1:20 (Figure 4B), showed that the apparent size of vesicles became smaller with greater quantities of the guest. If the formation of the proposed supramolecular polymer (Figure 5A) ensued, then nonstoichiometric quantities of the guest acted as "chain breakers" to alter the size/ morphology of vesicles to start resembling singly occupied $[1{\subset}2]$ baskets in size (Figure 3A). Moreover, pulse-field gradient (PFG) NMR spectroscopic measurements[63] of aqueous solution of **1** ($D^{(1)} = (1.58 \pm 0.02) \times 10^{-10}$ m[2]/s, Figure S9) containing one equivalent of **4** ($D^{(4)} = (4.50 \pm 0.01) \times 10^{-10}$ m[2]/s, Figure S9) showed that the apparent diffusion coefficients of guest ($D^{(1{\subset}4)} = (1.01 \pm 0.01) \times 10^{-10}$ m[2]/s) and host ($D^{(1{\subset}4)} = (0.91 \pm 0.07) \times 10^{-10}$ m[2]/s) are almost identical for equimolar mixtures (Figure S10). With the 3-fold excess of guest, however, the diffusion coefficients of the host ($D^{(1{\subset}4)} = (1.25 \pm 0.02) \times 10^{-10}$ m[2]/s, Figure S11) increased, to corroborate our DLS measurements manifesting a change in

the size of vesicles.[59] As in the case of linear AA−BB type supramolecular polymers,[62] the nonstoichiometric quantity of guest molecules is apparently disrupting the formation of two-dimensional and finite supramolecular polymers $[1 \subset 4]_n$ to, in this case, result in the formation of smaller vesicles via a reorganization of the material (Figure 5C).

At last, we decided to examine the complexation of paraquat **5** (Figure 6) with dual-cavity **1** since this dication is akin in
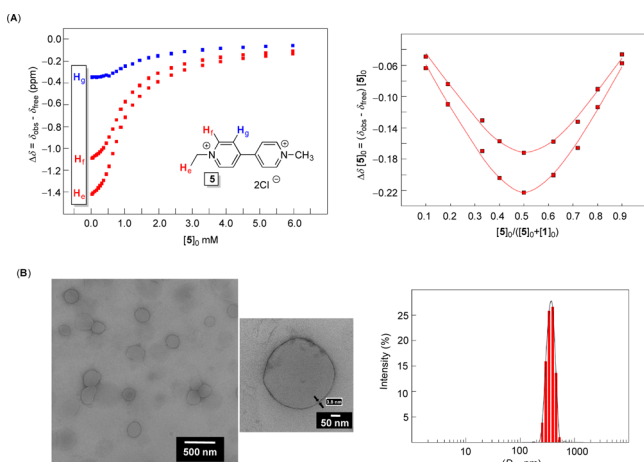


**Figure 6.** (A) The observed ¹H NMR chemical shifts ($\Delta\delta = \delta_{observed} - \delta_{free}$, ppm) of protons in **5** were obtained upon an incremental addition of its 12.0 mM solution to **1** (0.3 mM in D₂O) at 298.0 K. (Right) The Job plot corresponding to the formation of $[1 \subset 5]$ in D₂O at 298 K with $[1]_0 + [5]_0 = 0.3$ mM. (B) TEM images of a solution of **1** (0.2 mM in H₂O) containing **5** (0.2 mM) as deposited on a copper grid. (Right) Size distribution of **1** (0.2 mM in H₂O) containing one molar equivalent of **5** was obtained from DLS measurements at 298.0 K (PDI = 0.6).

shape and electronic characteristics to compound **4** (Figure 4). The two rod-shaped guests have positively charged nitrogen atoms separated by 7 and 10 Å, while their overall length is 10 and 15 Å (MMFFs, Spartan). Despite different lengths of **4** and **5**, dual-cavity **1** with negatively charged carboxylates at its surface was still expected to trap dicationic **5** in a multivalent fashion to give $[1 \subset 5]_n$ analogous to $[1 \subset 4]_n$ (Figure 5A): the methyl groups, instead of benzene rings could thus reside in the cavities of **1** to form favorable C−H⋯π contacts.[52] Indeed, NMR binding isotherms corresponding to the formation of $[1 \subset 5]_n$ (Figure 6A) are quite similar to those observed for $[1 \subset 4]_n$ (Figure 4A) with the greatest perturbation of resonances $H_e$ from two methyl groups in **5**. Evidently, these nuclei occupy the aromatic cavities of dual-cavity hosts, at the vesicular surface, thereby contributing to their large magnetic shielding. Dynamic light scattering and electron microscopy measurements, furthermore, revealed the formation of uni-lamellar vesicles whose size distribution is centered at 396 nm (Figure 6B). As the experimental results, indicating the formation of $[1 \subset 5]_n$ (Figure 6), are in line with those corresponding to $[1 \subset 4]_n$ (Figure 4), we deduce that curved and two-dimensional supramolecular polymers form in each case thereby attesting to the generality of the procedure. Interestingly, the apparent difference in the diameter of $[1 \subset 5]_n$ ($D_H = 396$ nm, Figure 5B) and $[1 \subset 4]_n$ ($D_H = 496$ nm) vesicles may indicate different packing densities of two-dimensional polymers arising from differently sized guests. Finally, paraquat is a widely used herbicide around the world and particularly

useful for limiting the proliferation of weed and grass.[64] It is, however, poisonous to both animals and humans with a prolonged exposure leading to the development of Parkinson's disease.[65] While there is no effective antidote for treating the poisoning with paraquat, this widely available substance remains a potential threat for its use in chemical warfare against both military and civilians. Modular dual-cavity baskets could, perhaps, mitigate the threat by permitting selective scavenging and/or detection of paraquat in aqueous media.[66]

## CONCLUSION

In summary, the formation of topologically novel and curved supramolecular polymers, embodying vesicles, can be achieved with dual-cavity baskets and bivalent guests. Since the recognition characteristics of our dual-cavity hosts could, perhaps, be tuned by varying the nature of amino acids at the rim,[67] we anticipate a potential use of this unique type of nanosized material for detecting and scavenging of organo-phosphorus chemical nerve agents, for which these dual-cavity baskets have some appreciable binding affinity.[4] The discovery could also be of interest for functionalization of liposomal surfaces,[68−71] comprising cavitands, and their additional stabilization. In fact, our preliminary studies with the entrapment of Rhodamine B in the reservoir of $[1 \subset 5]_n$ (Figure S12) confirm the formation of vesicles in addition to suggesting an increased stability of the vesicular system. The work is in progress and will be published in due course. Finally, one may employ the strategy for detecting polyvalent molecules[72−75] and as noted above removing toxic chemicals from the environment.[76]

## ASSOCIATED CONTENT

**Ⓢ Supporting Information**
The Supporting Information is available free of charge on the ACS Publications website at DOI: 10.1021/jacs.6b06562.

> Additional details of the experimental and computational protocols (PDF)

## AUTHOR INFORMATION

**Corresponding Author**
*badjic@chemistry.ohio-state.edu

**Notes**
The authors declare no competing financial interest.

## ACKNOWLEDGMENTS

## REFERENCES

(1) Hunter, C. A. *Angew. Chem., Int. Ed.* **2004**, *43*, 5310.
(2) Schneider, H. J. *Acc. Chem. Res.* **2015**, *48*, 1815.
(3) Raynal, M.; Ballester, P.; Vidal-Ferran, A.; van Leeuwen, P. W. N. M. *Chem. Soc. Rev.* **2014**, *43*, 1660.
(4) Sambrook, M. R.; Notman, S. *Chem. Soc. Rev.* **2013**, *42*, 9251.
(5) Wu, J.; Kwon, B.; Liu, W.; Anslyn, E. V.; Wang, P.; Kim, J. S. *Chem. Rev.* **2015**, *115*, 7893.
(6) Kim, S. K.; Sessler, J. L. *Acc. Chem. Res.* **2014**, *47*, 2525.

(7) Bistri, O.; Reinaud, O. *Org. Biomol. Chem.* **2015**, *13*, 2849.

(8) Brinker, U. H., Mieusset, J.-L., Eds.; *Molecular Encapsulation: Organic Reactions in Constrained Systems*; Wiley-VCH: Weinheim, Germany, 2010.

(9) Hof, F.; Craig, S. L.; Nuckolls, C.; Rebek, J., Jr. *Angew. Chem., Int. Ed.* **2002**, *41*, 1488.

(10) Sherman, J. C. *Tetrahedron* **1995**, *51*, 3395.

(11) Badjic, J. D.; Stojanovic, S.; Ruan, Y. *Adv. Phys. Org. Chem.* **2011**, *45*, 1.

(12) Yoshizawa, M.; Klosterman, J. K.; Fujita, M. *Angew. Chem., Int. Ed.* **2009**, *48*, 3418.

(13) Isaacs, L. *Acc. Chem. Res.* **2014**, *47*, 2052.

(14) Liu, S.; Gibb, B. C. *Chem. Commun.* **2008**, 3709.

(15) Kaphan, D. M.; Toste, F. D.; Bergman, R. G.; Raymond, K. N. *J. Am. Chem. Soc.* **2015**, *137*, 9202.

(16) Hermann, K.; Ruan, Y.; Hardin, A. M.; Hadad, C. M.; Badjic, J. D. *Chem. Soc. Rev.* **2015**, *44*, 500.

(17) Cram, D. J. *Science* **1988**, *240*, 760.

(18) Wittenberg, J. B.; Isaacs, L. *Supramol. Chem. Mol. Nanomater.* **2012**, *1*, 25.

(19) Cabot, R.; Hunter, C. A. *Chem. Soc. Rev.* **2012**, *41*, 3485.

(20) Rekharsky, M.; Inoue, Y. *Supramol. Chem. Mol. Nanomater.* **2012**, *1*, 117.

(21) Garde, S. *Nature* **2015**, *517*, 277.

(22) Diederich, F. *Mod. Cyclophane Chem.* **2005**, 519.

(23) Caceres, R. A.; Pauli, I.; Timmers, L. F. S. M.; Filgueira de Azevedo, W., Jr. *Curr. Drug Targets* **2008**, *9*, 1077.

(24) Zurcher, M.; Diederich, F. *J. Org. Chem.* **2008**, *73*, 4345.

(25) Quan, M. L. C.; Cram, D. J. *J. Am. Chem. Soc.* **1991**, *113*, 2754.

(26) Palmer, L. C.; Rebek, J., Jr. *Org. Biomol. Chem.* **2004**, *2*, 3051.

(27) Liu, F.; Wang, H.; Houk, K. N. *Sci. China: Chem.* **2011**, *54*, 2038.

(28) Cram, D. J.; Blanda, M. T.; Paek, K.; Knobler, C. B. *J. Am. Chem. Soc.* **1992**, *114*, 7765.

(29) Chapman, K. T.; Still, W. C. *J. Am. Chem. Soc.* **1989**, *111*, 3075.

(30) Barnard, A.; Smith, D. K. *Angew. Chem., Int. Ed.* **2012**, *51*, 6572.

(31) Branson, T. R.; Turnbull, W. B. *Chem. Soc. Rev.* **2013**, *42*, 4613.

(32) Fasting, C.; Schalley, C. A.; Weber, M.; Seitz, O.; Hecht, S.; Koksch, B.; Dernedde, J.; Graf, C.; Knapp, E.-W.; Haag, R. *Angew. Chem., Int. Ed.* **2012**, *51*, 10472.

(33) Mahon, E.; Barboiu, M. *Org. Biomol. Chem.* **2015**, *13*, 10590.

(34) Ren, C.; Zhang, J.; Chen, M.; Yang, Z. *Chem. Soc. Rev.* **2014**, *43*, 7257.

(35) Badjic, J. D.; Nelson, A.; Cantrill, S. J.; Turnbull, W. B.; Stoddart, J. F. *Acc. Chem. Res.* **2005**, *38*, 723.

(36) Breslow, R.; Belvedere, S.; Gershell, L.; Leung, D. *Pure Appl. Chem.* **2000**, *72*, 333.

(37) Mammen, M.; Chio, S.-K.; Whitesides, G. M. *Angew. Chem., Int. Ed.* **1998**, *37*, 2755.

(38) Kiessling, L. L.; Grim, J. C. *Chem. Soc. Rev.* **2013**, *42*, 4476.

(39) Yang, L.; Tan, X.; Wang, Z.; Zhang, X. *Chem. Rev.* **2015**, *115*, 7196.

(40) Chen, S.-G.; Yu, Y.; Zhao, X.; Ma, Y.; Jiang, X.-K.; Li, Z.-T. *J. Am. Chem. Soc.* **2011**, *133*, 11124.

(41) Appel, W. P. J.; Nieuwenhuizen, M. M. L.; Meijer, E. W. *Supramol. Polym. Chem.* **2012**, 3.

(42) Aida, T.; Meijer, E. W.; Stupp, S. I. *Science* **2012**, *335*, 813.

(43) Dong, R.; Zheng, Z.; Zhu, X.; Zhang, J.; Feng, X.; Pfeffermann, M.; Liang, H. *Angew. Chem., Int. Ed.* **2015**, *54*, 12058.

(44) Chen, S.; Yamasaki, M.; Polen, S.; Gallucci, J.; Hadad, C. M.; Badjic, J. D. *J. Am. Chem. Soc.* **2015**, *137*, 12276.

(45) Hunter, C. A.; Anderson, H. L. *Angew. Chem., Int. Ed.* **2009**, *48*, 7488.

(46) Zhang, Z.; Luo, Y.; Chen, J.; Dong, S.; Yu, Y.; Ma, Z.; Huang, F. *Angew. Chem., Int. Ed.* **2011**, *50*, 1397.

(47) Haino, T. *Polym. J.* **2013**, *45*, 363.

(48) Castellano, R. K.; Rudkevich, D. M.; Rebek, J., Jr. *Proc. Natl. Acad. Sci. U. S. A.* **1997**, *94*, 7132.

(49) Israelachvili, J. N., Ed.; *Intermolecular and Surface Forces*; Elsevier: Amsterdam, The Netherlands, 2011.

(50) Shimizu, T.; Masuda, M.; Minamikawa, H. *Chem. Rev.* **2005**, *105*, 1401.

(51) Chen, S.; Ruan, Y.; Brown, J. D.; Gallucci, J.; Maslak, V.; Hadad, C. M.; Badjic, J. D. *J. Am. Chem. Soc.* **2013**, *135*, 14964.

(52) Chen, S.; Ruan, Y.; Brown, J. D.; Hadad, C. M.; Badjic, J. D. *J. Am. Chem. Soc.* **2014**, *136*, 17337.

(53) Marrink, S. J.; Tieleman, D. P. *Chem. Soc. Rev.* **2013**, *42*, 6801.

(54) Badjic, J. D.; Kostic, N. M. *J. Phys. Chem. B* **2000**, *104*, 11081.

(55) Dominguez, A.; Fernandez, A.; Gonzalez, M.; Iglesias, E.; Montenegro, L. *J. Chem. Educ.* **1997**, *74*, 1227.

(56) Yan, Q.; Zhou, R.; Fu, C.; Zhang, H.; Yin, Y.; Yuan, J. *Angew. Chem., Int. Ed.* **2011**, *50*, 4923.

(57) Yoshizawa, T.; Mizoguchi, M.; Iimori, T.; Nakabayashi, T.; Ohta, N. *Chem. Phys.* **2006**, *324*, 26.

(58) Stojanovic, S.; Turner, D. A.; Share, A. I.; Flood, A. H.; Hadad, C. M.; Badjic, J. D. *Chem. Commun.* **2012**, *48*, 4429.

(59) Ruan, Y.; Chen, S.; Brown, J. D.; Hadad, C. M.; Badjic, J. D. *Org. Lett.* **2015**, *17*, 852.

(60) Hirose, K. *Anal. Methods Supramol. Chem.* **2007**, 17.

(61) Arduini, A.; Pochini, A.; Secchi, A. *Eur. J. Org. Chem.* **2000**, *2000*, 2325.

(62) Burke, K. A.; Sivakova, S.; McKenzie, B. M.; Mather, P. T.; Rowan, S. J. *J. Polym. Sci., Part A: Polym. Chem.* **2006**, *44*, 5049.

(63) Cohen, Y.; Avram, L.; Frish, L. *Angew. Chem., Int. Ed.* **2005**, *44*, 520.

(64) Gawarammana, I. B.; Buckley, N. A. *Br. J. Clin. Pharmacol.* **2011**, *72*, 745.

(65) Kamel, F. *Science* **2013**, *341*, 722.

(66) Yu, G.; Zhou, X.; Zhang, Z.; Han, C.; Mao, Z.; Gao, C.; Huang, F. *J. Am. Chem. Soc.* **2012**, *134*, 19489.

(67) Ruan, Y.; Dalkilic, E.; Peterson, P. W.; Pandit, A.; Dastan, A.; Brown, J. D.; Polen, S. M.; Hadad, C. M.; Badjic, J. D. *Chem. - Eur. J.* **2014**, *20*, 4251.

(68) Voskuhl, J.; Ravoo, B. J. *Chem. Soc. Rev.* **2009**, *38*, 495.

(69) Lee, H.-K.; Park, K. M.; Jeon, Y. J.; Kim, D.; Oh, D. H.; Kim, H. S.; Park, C. K.; Kim, K. *J. Am. Chem. Soc.* **2005**, *127*, 5006.

(70) Ludden, M. J. W.; Reinhoudt, D. N.; Huskens, J. *Chem. Soc. Rev.* **2006**, *35*, 1122.

(71) Mulder, A.; Huskens, J.; Reinhoudt, D. N. *Org. Biomol. Chem.* **2004**, *2*, 3409.

(72) Paleos, C. M.; Pantos, A. *Acc. Chem. Res.* **2014**, *47*, 1475.

(73) Vorup-Jensen, T. *Adv. Drug Delivery Rev.* **2012**, *64*, 1759.

(74) Mueller, M. K.; Brunsveld, L. *Angew. Chem., Int. Ed.* **2009**, *48*, 2921.

(75) Lowe, J. N.; Fulton, D. A.; Chiu, S.-H.; Elizarov, A. M.; Cantrill, S. J.; Rowan, S. J.; Stoddart, J. F. *J. Org. Chem.* **2004**, *69*, 4390.

(76) Teresa Albelda, M.; Frias, J. C.; Garcia-Espana, E.; Schneider, H.-J. *Chem. Soc. Rev.* **2012**, *41*, 3859.